Efficiency of a Community-Scale Borehole Thermal Energy Storage Technique for Solar Thermal Energy

Ronglei Zhang[1], Ning Lu[2] and Yu-shu Wu[3]

[1]PhD Student, Energy Modeling Group, Department of Petroleum Engineering, Colorado School of Mines, Golden, Colorado, 80401, USA; PH (303) 384-2370; email: rozhang@mines.edu
[2]Professor, Division of Engineering, Colorado School of Mines, Golden, Colorado, 80401, USA; PH (303) 273-3654; FAX: (303) 273-3602; email: ninglu@mines.edu
[3]Professor, Energy Modeling Group, Department of Petroleum Engineering, Colorado School of Mines, Golden, Colorado, 80401, USA; PH (303) 384-2093; FAX: (303) 273-3189; email: ywu@mines.edu

ABSTRACT: Solar thermal has been quite efficient in harvesting solar energy, but has not been used widely at the community-scale as thermal energy is difficult to store. Borehole thermal energy storage (BTES) has been recently researched by several countries for its suitability in storing excess heat generated from solar thermal panels during the summer times. The first community-scale BTES system in North America was installed in the town of Okotoke, Alberta, Canada in 2006 in order to supply partial winter heating energy for 52 residual houses. To better understand the working principles of BTES and to improve BTES performance for future applications at larger scales, a three-dimensional heat transfer model is established, using the 5-year in-situ monitoring data. The model realistically imposes the time-dependent heat injection and withdrawals rates measured at the site. A total of 10 continuous years of annual cycle are simulated. The modeling results are compared with the measured temperature data over the simulation times and space. The time-dependent temperature distributions within the borehole region agree well with the measured temperature profiles. The predicted energy recovery efficiency approaches to 27% after 10 years, which also compares well with the current year efficiency of 25% at the site.

1. Introduction

The Drake Landing Solar Community (DLSC) is the first community-scale borehole solar thermal energy storage (BTES) system in North America. It is located in the Town of Okotoke, Alberta, Canada (McDowell and Thornton, 2008) and connects 52 detached energy-efficient houses within the subdivision (Sibbitt et al., 2007). The BTES system is designed to supply more than 90% of the space heating requirements with solar energy (Sibbitt et al., 2007; McDowell and Thornton, 2008). The entire DLSC's BTES system is shown in Figure 1 and consists of an 800-panel garage mounted array of solar collectors, an energy center for short-term thermal storage (STTS) tanks, and an underground BTES space. The system was designed to reach a 90% annual solar fraction after 5 years of operation. The system started to live in fall 2006.

While it was reported that a computer simulation was first done for the entire DLSC system during the design phase (McDowell and Thornton, 2008) and later by McDowell and Thornton (2008), it is not clear if any detailed simulations of full-scale three-dimensional underground BTES space fluid flow and heat transfer model has ever been established. Also, the governing parameters regarding the annual efficiency of BTES have not been well studied. Therefore, the objectives of this paper are: (1) to establish a 3D full-scale numerical model for fluid flow (in the circulation loop) and heat transfer of the BTES at DLSC sites, (2) to validate the model against the collected temperature data, and (3) to predict the efficiency of the BTES for 10 years.

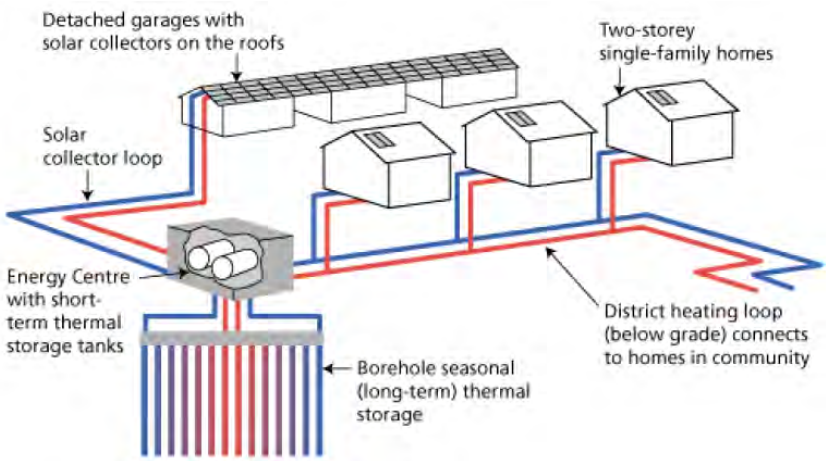

Figure 1. Sketch of a simplified BTES system at DLSC (Sibbitt et al., 2007).

2. The Performance of Subsurface BTES System

2.1 BTES System Configuration

The subsurface BTES site has the dimension of 30 m (long) × 30 m (wide) × 35 m (deep), as shown in Figure 2a. It consists of 144 boreholes, each 35 m deep. The spacing between adjacent boreholes is uniformly around 2.25 m. The diameter of the boreholes is 0.11 m. All boreholes are inter-connected in 24 series through U-tubes in Figure 2b. Each series has 6 boreholes connecting the injection/withdrawal from the center to the outer boundary roughly along the radial direction. When the solar collector system produces more heat in summers, hot water will be pumped to the center borehole, while the reverse is the case when heat is needed for home space heating in winters. Thus, one quarter of the entire BTES system can be simulated to represent the whole system, consisting of 6 series and forming a loop with hot water flowing in (in summer times) or out (in winter times) from the center and cooler water flowing out (in summer times) or in (in winter times) at the outer end.

2.2 Transient Performance of BTES system

The total charging/discharging flow rate from August 1, 2009 to July 30, 2010 fluctuates closely around 2.6 l/s (or 0.108 kg/s per circulation loop), as shown in Figure 3a. The flow rate does drastically reduce occasionally from time to time, but has negligible effect on the average flow rate estimation.

The injection and withdrawal temperature at the center of the BTES for the entire 12-month cycle is shown in Figure 3b. The time series still begins at March 1, 2010. As shown, temperature fluctuates within a day for up to 15 °C. Nevertheless, a pattern can be delineated; temperature fluctuates around 50 °C from March to June, around 65 °C from July to September, and around 45 °C from October to February. Therefore, the charging period starts roughly from March to September, and the discharging period starts roughly from October to February.

The blue and red dots in Figure 2a show the temperature monitoring points near the ground surface of one circulation loop. The temperature output from the monitoring point (see Figure 2c) reflects temperature changes at the inlet and outlet points of every borehole. The total length of one circulation loop with 6-borehole series is 432 m from the center of the field to the outer end over the horizontal distance of 15 m. During hot water injection (charging) period, temperature at the center of the field is generally the highest and gradually decreases as the water

moves down-and-up in each loop. This pattern can be seen from the measured temperature as a function of the travel distance in the water loop and times in Figure 4 for the months in charging period and discharging period.

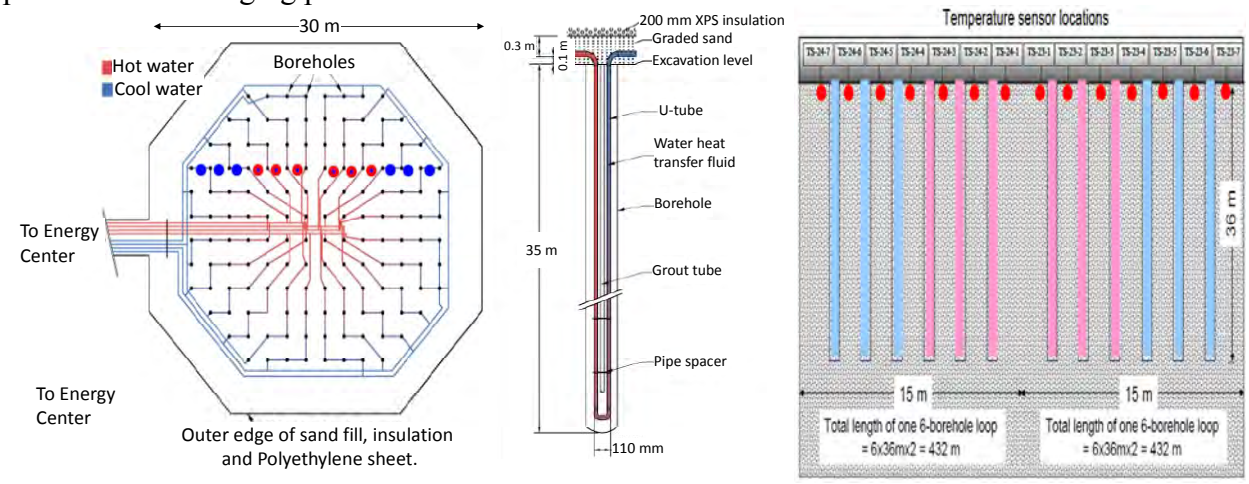

(a) (b) (c)

Figure 2. BTES system at DLSC site: (a) plan view, (b) single borehole configuration, and (c) temperature monitoring points along the vertical cross. (Sibbitt et al., 2007)

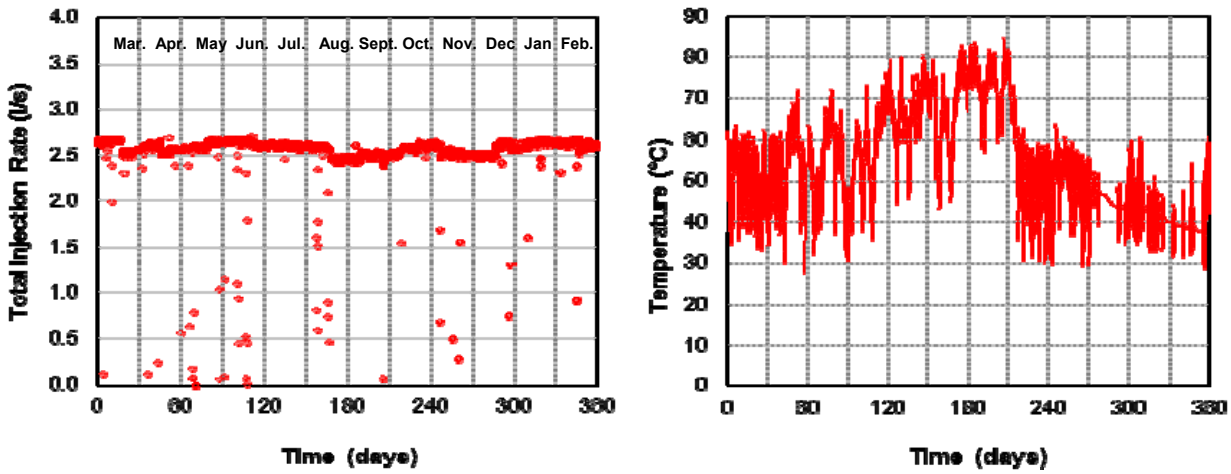

(a) (b)

Figure 3. (a) Total Charging/discharging flow rate near the center location of the BTES. (March 1, 2010 is the beginning day of charging period), (b) Charging/discharging temperature performance at a monitoring point.

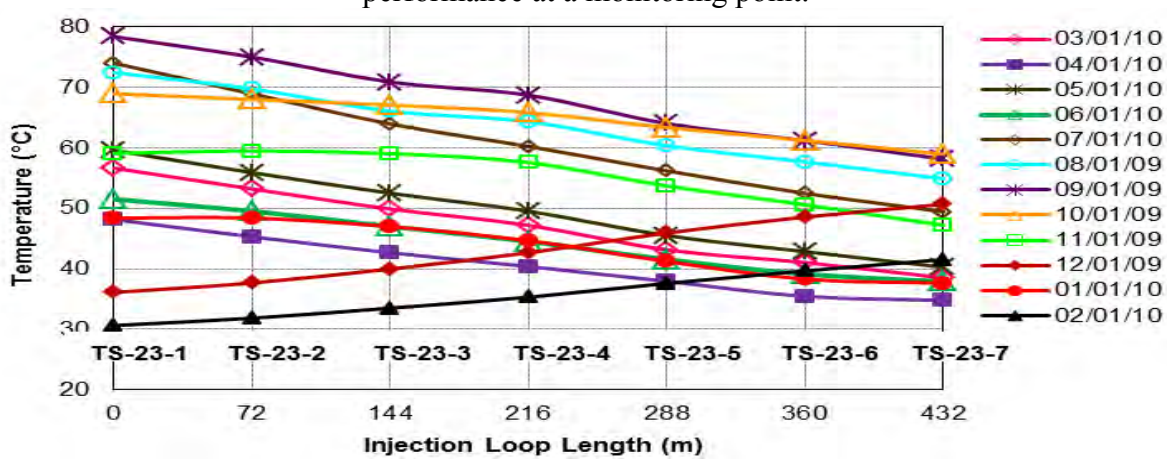

Figure 4. Measured temperature profile at the monitoring points.

3. Numerical Modeling Approach

3.1 Numerical Simulator

TOUGH2 simulator (Pruess, 1991) is employed to carry out the present simulations. It simulates non-isothermal, multi-components and multiphase fluid flow in porous or fractures media. The module EOS3, which simulates the flow of water, air and heat, is used for subsurface BTES model at the DLSC site. All water properties in EOS3 module are represented by the steam table equations as given by the International Formulation Committee (1987). The flow and transport in geologic media are based on space discretization by means of integral finite differences (Narasimhan and Witherspoon, 1976). A fully implicit scheme of finite differencing in time is adopted. At each time step, and for each volume element, the model solves for three mass balance equations for three components (i.e. water, air and heat).

3.2 Numerical Model

A plan view of the site and the borehole array are shown in Figure 2a. The block of the boreholes has dimensions of 30 m (long) ×30 m (wide) ×35 m (deep). By symmetry of the borehole array, one quarter of the domain is necessary for numerical simulations. Therefore, only 36 boreholes with 6 borehole series are simulated. The borehole region, therefore, represents a volume of 8,100 m^3 with dimensions of 15 m (long) ×15 m (wide) ×36 m (deep). The three-dimensional finite difference discretization of the domain and the imposed boundary condition is shown Figure 5a, which has a volume of 150,000 m^3 with dimensions of 50 m (long) ×50 m (wide) ×60 m (deep). The simulated domain has 30 grids in the *x*-horizontal direction, 20 grids in the *y*-horizontal direction, and 8 grids in the *z*-vertical direction. The connectivity of all 36 boreholes follows the true in-situ arrangement and is shown in Figure 5b. In addition, all boreholes are simulated with square shape cross-section areas equal to the real dimension of the circular shape boreholes (see Figure 5c). The square shape borehole is divided into inner and outer elements. Between them, there is no hydrological and thermal connection, except at the bottom. The hot water is pumped in or out from the top of the outer element, passes through the bottom where the two are connected, and flows out or in at the top of the inner element.

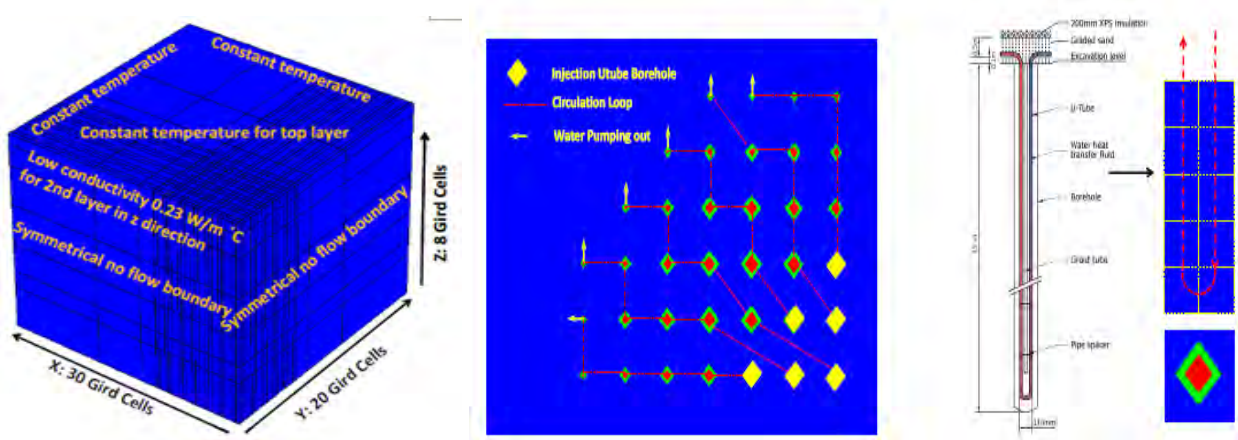

(a) (b) (c)

Figure 5. Sketches of: (a) discretized 3D model, (b) borehole connection pattern and (c) discretized U-tube boreholes connection.

Based on the transient data of BTES site, the flow directions changed several times a day, making it difficult to setup a true time dependent flow rate for the numerical modeling. However,

several patterns of switch are clear; (1) in the months of May to September, charging is the predominating mode, (2) in the months of October to February, discharging is the predominating mode, and (3) in the months of March and April, both charging and discharging are considerable. The whole BTES site is assumed to be a dependent insulation system and no heat exchange with atmosphere. The heat injected during the charging period can be withheld in the range the site. Therefore, the short charging/discharging period can be incorporated into predominating period under the condition that the total charging/discharging days are constant.

Based on these switching patterns and injection temperature and rates, the charging and discharging periods are divided into 21 periods over the entire year, as shown in Table 1. To ensure the overall heat injection and withdrawal to be representative and accurate for energy balance, the following energy equivalency equation is used to calculate the average temperatures for each of those 21 periods $T_{i\text{-}ave}$:

$$T_{i-ave} = \frac{\sum_{j=1}^{n} T_j Q_j \Delta t_j c_w}{\sum_{j=1}^{n} Q_j \Delta t_j c_w} \tag{1}$$

where index i represents the period number from 1 to 21, index j represents the jth data point within the period i, T_j is the measured temperature, Q_j is the measured flow rate, Δt_j is the jth time interval for the injection/withdrawal, and c_w is the specific heat of water injected.

The result of the above calculation is shown in Figure 6, which correctly represents the total charging period of 165 days, the total discharging period of 84 days, and the dormant (no flow) period of 116 days during the one year measurement period.

Table 1. Simulated flow rate, temperature, enthalpy and duration.

Time (d)	Flow rate(kg/s)	Injection temperature(°C)	*Enthalpy(J/kg)	Injection scheme
12	0.108	58.940	2.74630E+05	charging
14	0.108	27.500	1.28136E+05	discharging
37	0.000	---	---	no injection
55	0.108	59.020	2.75003E+05	charging
62	0.000	---	---	no injection
67	0.108	30.477	1.42007E+05	discharging
87	0.108	58.188	2.71126E+05	charging
92	0.000	---	---	no injection
122	0.108	59.030	2.75049E+05	charging
153	0.108	67.920	3.16472E+05	charging
184	0.108	68.530	3.19314E+05	charging
214	0.108	74.730	3.48203E+05	charging
218	0.108	63.830	2.97415E+05	charging
228	0.108	32.850	1.53064E+05	discharging
245	0.000	---	---	no injection
249	0.108	57.670	2.68712E+05	charging
269	0.000	---	---	no injection
298	0.108	33.870	1.57817E+05	discharging
313	0.000	---	---	no injection
351	0.108	33.870	1.57817E+05	discharging
365	0.000	---	---	no injection

**The enthalpy values of hot water are inferred from the Steam Table Calculation as given by the International Formulation Committee (1987).*

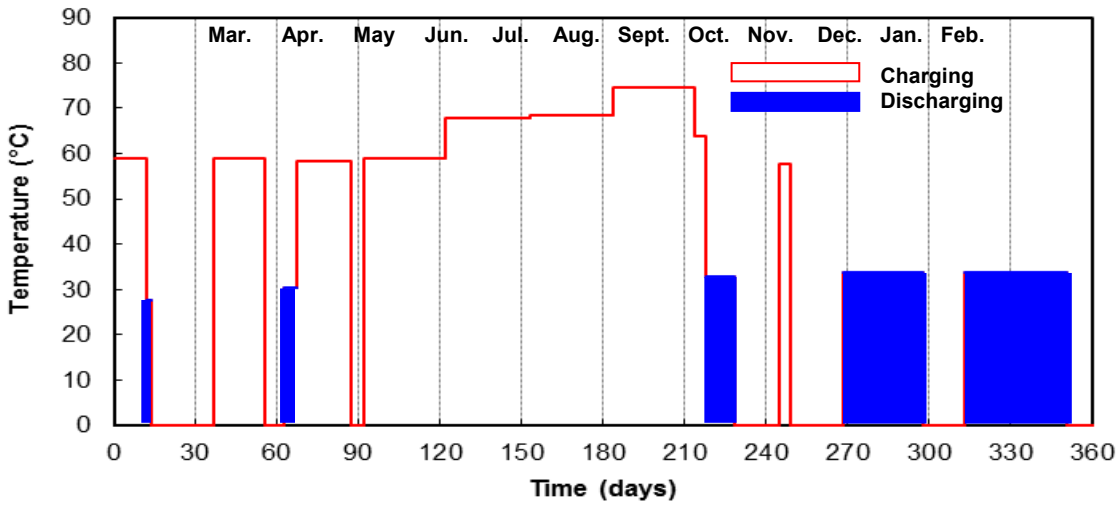

Figure 6. Averaged temperature and time intervals for charging/discharging period.

3.2.3 Boundary condition and data initialization

For the simulated domain, the following boundary conditions are imposed in order to better represent the in-situ conditions. An atmosphere temperature (15 ºC) is specified at the two far field boundaries and at both top and bottom boundaries. To represent the insulation feature on the top, two layers of low thermal conductivity material (0.23 w/m· °C) are used. By symmetry, no-heat flow boundary condition is imposed on the vertical planes cross the center of the BTES site. For the soil properties in numerical model, the permeability of the injection boreholes is set to be 10^{-10} m^2, and the permeability of the surrounding soil is set to be 10^{-19} m^2. The permeability of borehole grid cell is 10^9 times as that of surrounding soil for no fluid transportation between injection borehole and surrounding soil. The porosity of borehole domain is set to be zero for the void space in the U-shape borehole of BETS sites. All the material properties are summarized in Table 2.

Table 2. Initialization data for the 3D fluid flow and heat transfer model.

Parameter	Value	Unit
Soil permeability	10^{-19}	m^2
Initial pressure	1.000	bar
Soil porosity	0.250	unitless
Initial temperature	15.00	°C
Injection rate	0.108	kg/s
Soil thermal conductivity	2.030	w/m·°C
Borehole radius	0.055	m
Borehole (U-tube) hydraulic conductivity	10^{-10}	m^2
Heat conductivity(insulation dry sand)	0.230	w/m·°C
Borehole porosity (U-tube)	1.000	unitless

4. Results and Discussion

4.1 Full Scale Temperature Contour

The numerical simulation for the established 3D model is carried out for continuous 10 years. Temperature and flow rate in Table 1 are used as the annual cycle for 10 cycles (years) in the simulations. The starting date is hypothetical set to be March 1, 2006. The evolution of 3D temperature contours and 2D plane temperature contour at the end of charging period (the end of September) and discharging period (the end of February) are selected for 1st year, 3rd year and 10th year as shown in Figure 7.

Several semi-quantitative observations can be made from Figure 8. In the 1st year, the elevated temperature region is restrained within the borehole region (30 m < X < 50 m, Y < 15 m, Z < 40 m). The elevated temperature within this region is in the 50's °C at the end of charging period (0.58 year or end of September). Around the end of discharging period (0.96 year or end of February), the elevated temperature is in the 30's °C. As time elapses, the elevated temperature region expands both outward and downward and the average temperature increases at the same day each year (refer to temperature contours during 1st year, 3rd year and 10th year). At the end of September in the 3rd year, which is equivalent to September 30 2009, the elevated temperature in the borehole region (30 m < X < 50 m, Y < 15 m, Z < 40 m) is in 60's °C, about 10 °C higher than that at the same time in the 1st year. Correspondingly, at the end of discharging period (2.96 year or February 28 2010), the elevated temperature in the borehole region is in 40's °C, about10 °C higher than that at the end of February in the 1st year. The elevated region now expands to 25 m in the *y*-direction and 45 m in the *z*-direction. By the end of the 10th year, the affected region has just about to reach the model boundaries. During this year, at the end of September, temperature within the borehole region reaches 70's °C at the depth of 25 m, which is about 20 °C higher than that at the same day in the 1st year. Correspondingly, at the end of discharging period (9.96 year or February 28 2017), the elevated temperature in the borehole region is in 50's °C, which is about 20 °C higher than that at the end of February in the 1st year. The temperature distribution during the discharging period is much more uniformly distributed than that during the charging period within the borehole region.

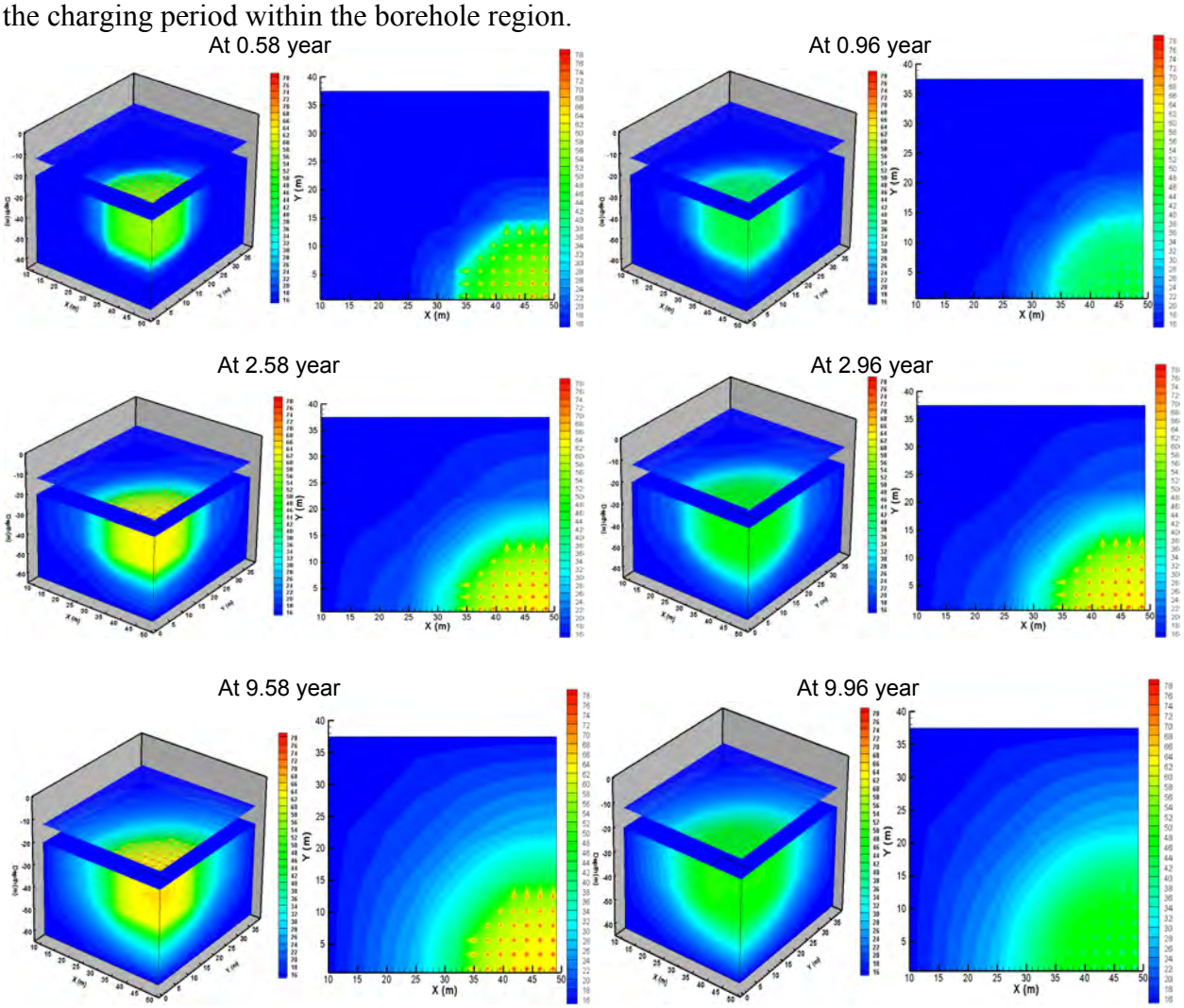

Figure 7. Full scale temperature contours at the end of charging/discharging periods.

4.2 Transient Temperature Profile Comparison

The comparisons between field data and simulation results are employed to illustrate the spatial and temporal temperature distributions between simulated and measured data. Two dates of a year are selected to be representative for the comparisons: September 28 (at the end of the continuous charging period) and February 19 (at the end of the continuous discharging period). Horizontal temperature profiles on these dates in the first 5 years of the simulations along with the measured temperature profiles in approximately the same locations are shown in Figure 8.

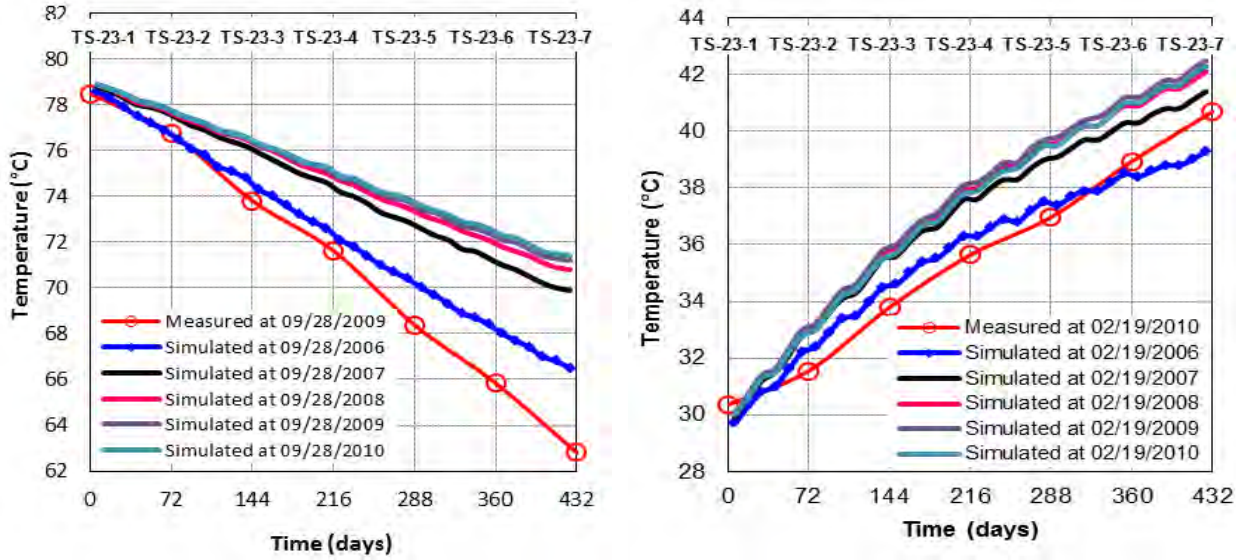

(a) (b)

Figure 8. Temperature profiles along one circulation loop at two representative dates.

On September 28, 2009, which is at the end of the continuous charging period, the measured temperature profile shows a nearly linear distribution in temperature decreasing from a maximum of 78.5 °C near the center location (0 m, in Figure 8a) to a minimum of 62.8 °C near the end of the loop (432 m). The simulated temperature profile on September 28 of 2006 shows nearly linear distribution in temperature decreasing from a maximum of 78.9 °C near the center location to a minimum of 66.5 °C near the end of the loop (432 m). The simulated temperature profile compares very well with the measured temperature for the loop length < 216 m. At the end of the loop (432 m), the model overestimates the measured temperature by 3.7 °C, which might indicate the ambient and initial temperature of 15.0 °C could be a little higher than the realistic one at BTES site of Canada. On September 28, 2010, the simulated temperature profile continues to be upward shifting yet reaches an asymptotical value of 71.4 °C at the end of the loop. This is 8.6 °C above the measured temperature at this point. However, the measured temperature near the center location remains closely with the measured temperature for within 0.4 °C.

On February 19, 2010, which is at the end of the continuous discharging period, the measured temperature profile shows a nearly linear distribution in temperature increasing from a minimum 30.4 °C near the center location (0 m, in Figure 8b) to a maximum temperature of 40.7 °C near the end of the loop (432 m). This date marks the lowest energy level in the BTES system of a year. The simulated temperature profile on February 19 of 2006 shows nearly linear distribution in temperature increasing from a minimum temperature of 30.0 °C near the center location to a maximum of 39.8 °C near the end of the loop (432 m). The simulated temperature profile

compares very well with the measured temperature over the entire loop length with temperature difference < 1.4 °C. At the end of the loop (432 m), the model underestimates the measured temperature by 1.4 °C. On February 19, 2010, the simulated temperature profile continues to be upward shifting yet reaches an asymptotical value of 42.3 °C at the end of the loop. This is 1.6 °C above the measured temperature at this point. Overall the temperature profile accords very well with the measured one.

4.3 Efficiency Calculation

The annual overall efficiency E in the heat recovery of the underground BTES space at the DLSC site can be assessed by computing the total heat extracted from the BTES space during the discharging period and the total heat injected into the BTES space, namely:

$$E = \frac{\sum_{j=1}^{n} S_j Q_j \Delta t_j}{\sum_{j=1}^{m} S_j Q_j \Delta t_j} \tag{2}$$

where S_j is the enthalpy of hot water that can be found from the steam table and are shown in Table 1, n is the total discharging segments during the entire discharging period, and m is the total charging segment during the entire charging period. The annual overall efficiency for the 10-year simulations is plot in Figure 9. It can be seen that the predicted first year's efficiency is about 7%, the second year 17%, the third year 21%, the fourth year 23%, and the fifth year 24%. Eventually, it flats out at around 27%. Based on personal communication with Dr. Wong of SAIC, the past year's efficiency is around 25%, which accords well with the fifth year prediction in the simulations. The agreement is within 4%, i.e., 25% vs. 24%.

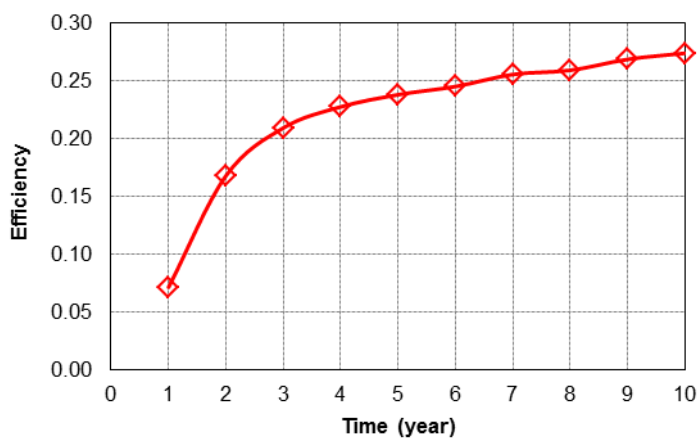

Figure 9. Simulations of the efficiency of the BTES system for 10 years.

Conclusions

1. A 3D full-scale numerical model for the subsurface BTES system at the DLSC site is established, and the model realistically imposes the time-dependent heat injection and withdrawals rates measured at the site. The simulation of transient fluid flow and heat transfer in the model is carried out by EOS3 Module of TOUGH2 family code.

2. A total of 10 continuous years of annual cycle are simulated. The modeling results are compared with the measured temperature data over the simulation times and space. The time-

dependent temperature distributions within the borehole region agree well with the measured profiles.

3. For the region around the end of the loop, considerable differences in temperature between the measured and simulated are found. The difference is in the range of 0.4 to 8.7 °C above the measured temperature and is attributed to the difference between the imposed initial temperature (15 °C) and the in-situ ambient temperature prior to the BTES operation at the DLSC site.

4. The final efficiency value of the DLSC BTES site is predicted to be around 27%. The error resulted from a higher ambient temperature should have a minimum impact on the recovery energy efficiency of the model, which is confirmed by the comparison between the computed efficiency and the reported efficiency, which is within 4% in difference.

Acknowledgments

We are grateful to Dr. Bill Wong of SAIC, Canada for fruitful discussions and for kindly providing temperature and flow rate data. Special thanks go to Dr. Jay Burch of National Renewable Energy Laboratory (NREL) for his valuable comments. This work was supported by NREL.

References

International Formulation Committee. (1987). "A Formulation of the Thermodynamic Properties of Ordinary Water Substance." *IFC Secretariat*, Düsseldorf, Germany.

McDowell, T.P., and Thornton, J.W. (2008). "Simulation and model calibration of a large-scale solar seasonal storage system." *The Third National Conference of IBPSA-USA*, Berkeley, California, July 30-August 1.

Narasimhan, T.N., Witherspoon, P.A. (1976). "An integrated finite difference method for analyzing fluid flow in porous media." *Water Resour. Res.* 12, 57–64.

Pruess, K. (1991). "TOUGH2: A General-purpose Numerical Simulator for Multiphase Fluid and Heat Flow." *Lawrence Berkeley Laboratory*, LBL-29400, Berkeley, CA.

Sibbitt, B., Onno, T., McClenahan, D., Thornton, J., Brunger, J., Wong, B. (2007). "The Drake Landing solar community project – early results." *Canadian Solar Buildings Conference*, Calgary, June 10-14.